

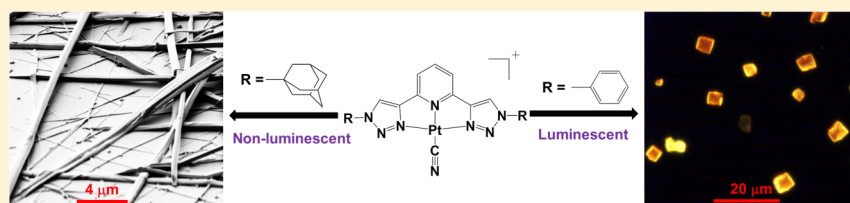
Tuning the Structural and Photophysical Properties of Cationic Pt(II) Complexes Bearing Neutral Bis(triazolyl)pyridine Ligands

Naveen Kumar Allampally,^{†,‡,⊥} Constantin-Gabriel Daniliuc,[§] Cristian A. Strassert,^{*,‡} and Luisa De Cola^{*,†,‡,||}

[†]NRW Graduate School of Chemistry, [‡]Center for Nanotechnology (CeNTech) and Physikalisches Institut, and

[§]Organisch-Chemisches Institut, Westfälische Wilhelms-Universität Münster, 48149 Münster, Germany

Supporting Information



ABSTRACT: The emission properties of a series of cationic Pt(II) complexes bearing neutral tridentate 2,6-bis-(1H-1,2,3-triazol-5-yl)pyridine and monoanionic ancillary ligands (Cl^- or CN^-) are described. By varying the substitution pattern on the 1,2,3-triazole moieties of the tridentate luminophore and the nature of the ancillary ligand, we were able to tune the intermolecular interactions between the complexes and therefore the electronic interactions between the metal centers. Indeed, all the compounds possessing Cl^- as ancillary ligand are nonluminescent at room temperature, while the complexes containing CN^- are luminescent. Interestingly, the π -accepting nature of this ancillary ligand induces Pt(II)–Pt(II) interactions irrespectively of bulky substitution patterns on the tridentate ligand.

INTRODUCTION

Platinum complexes have attracted a lot of interest for many fundamental and applied aspects that range from electronics^{1–10} to sensing,^{11–17} medicine,^{18–31} and bioimaging.^{32–37} In particular, cisplatin has been introduced in oncology for the treatment of diverse classes of cancer.^{28,38,39} To improve the selectivity and efficacy of these complexes toward malicious tumors, intensive studies have been devoted to the modification of the ligands coordinated to the platinum center.^{28,40–42} An alternative strategy consists of using Pt(IV) derivatives as a *prodrug* and to reduce the complex in vivo to the toxic Pt(II) species.⁴³ In addition, cationic Pt(II) complexes have been used as intercalators for duplex and G-quadruplex DNA.^{19,22,44–49} Cationic complexes have also been employed for preparing luminescent Langmuir–Blodgett films by attaching alkyl chains of suitable length on the coordinated tridentate ligand taking advantage of the aggregation properties of these square planar systems.⁵⁰ Indeed, their tendency to self-assemble has been also exploited to form various aggregates,⁵¹ fibers,^{52,53} gels,^{54,55} liquid crystals,^{56–59} and micelles.⁶⁰ Recently, microcrystalline structures of cationic ($\text{N}^{\wedge}\text{N}^{\wedge}\text{N}$)-Pt(II) complexes have been created and used for improving the efficiency of electronic device performances, such as field effect transistors (FET).^{61–66} As these self-assembled structures are highly ordered and can possess strong metal–metal interactions between adjacent molecules, conductivity can be modulated by exposure to vapors, which can influence the packing.⁶⁷ In general, ($\text{N}^{\wedge}\text{N}^{\wedge}\text{N}$)-Pt(II) complexes with chloride as ancillary ligands are nonluminescent at room temperature (rt) in

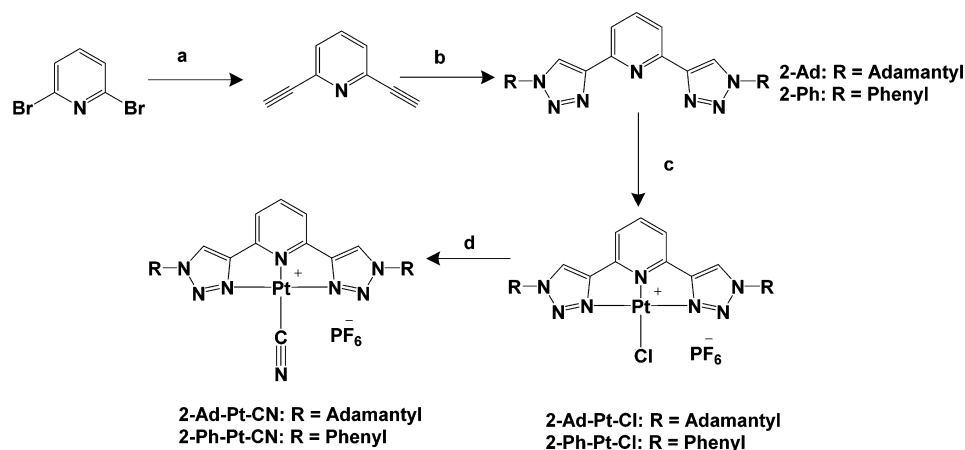
solution, since the d–d metal-centered (MC) excited states, which are thermally accessible, dissipate the energy by nonradiative decay.³⁶ To turn the luminescence on, stronger ancillary ligands are required, as well as the replacement of one of the N atoms of the tridentate ligand by a cyclometalating atom. These two approaches can effectively push the MC states to higher energies, yielding phosphorescence at rt.

Herein, we describe the synthesis of substituted 2,6-bis-(1H-1,2,3-triazol-5-yl)pyridine derivatives and the resulting cationic ($\text{N}^{\wedge}\text{N}^{\wedge}\text{N}$)-Pt(II) complexes bearing CN^-/Cl^- as ancillary ligands, their structural features, the morphology of the self-assembled structures, and the photophysical properties. We chose two different types of substituents on the tridentate ligand, namely, bulky adamantyl (Ad) and planar phenyl (Ph) moieties. Interestingly, replacement of Cl^- on Pt(II) by CN^- turns on the phosphorescence in powders and neat films, thus enabling the photophysical characterization. Furthermore, we also created self-assembled micro/nano structures of the complexes by following a reprecipitation method,⁶¹ and their morphologies are investigated.

RESULTS AND DISCUSSION

Compounds $\text{Pt}(\text{DMSO})_2\text{Cl}_2$ (DMSO = dimethyl sulfoxide), 2,6-diethynylpyridine (**1**),⁶⁸ 2,6-bis(4-(adamantan-1-yl)-1H-1,2,3-triazol-5-yl)pyridine (**2-Ad**), 2,6-bis(4-phenyl-1H-1,2,3-triazol-5-yl)pyridine (**2-Ph**), and the ($\text{N}^{\wedge}\text{N}^{\wedge}\text{N}$)Pt(II)CN

Received: October 26, 2014

Scheme 1^a

^a(a) (i) Ethynyltrimethylsilane, Pd(PPh₃)₄, Cu(I), NEt₃, toluene, overnight, 40 °C under N₂ atmosphere and (ii) KOH, MeOH/H₂O, stir at rt overnight, yield 63%. (b) For **2-Ad**: CuBr, *N,N,N',N',N'*-pentamethyl diethylenetriamine, 1-azidoadamantane, dry THF, stir at rt for 24 h under N₂ atmosphere, yield 72%. For **2-Ph**: CuSO₄·5H₂O, sodium ascorbate, *t*-BuOH/H₂O, azidobenzene, stir at rt for 24 h, yield 80%. (c) (i) Pt(DMSO)₂Cl₂, dry MeOH, reflux under N₂ atmosphere for 48 h and (ii) anion exchange with NH₄PF₆. (d) AgCN, ACN, 65 °C, under N₂ atmosphere for 4 h.

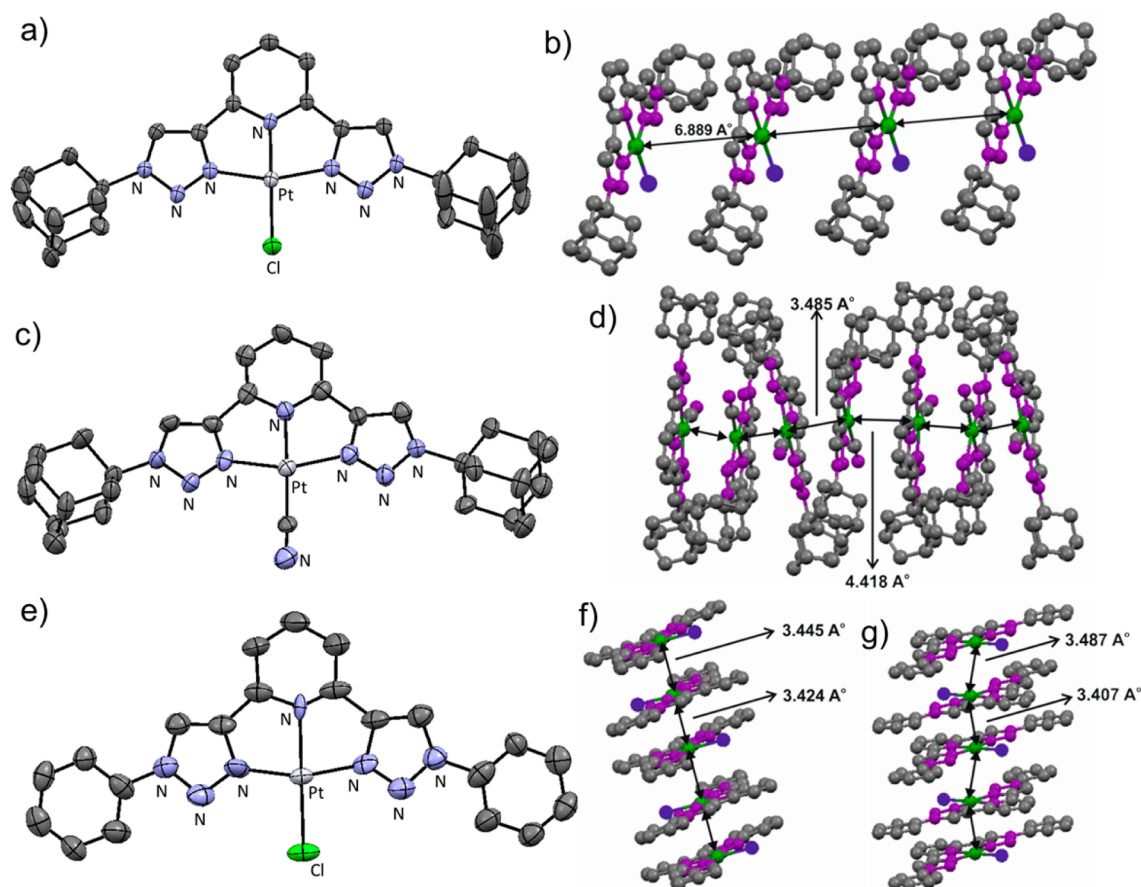


Figure 1. Structure of the complexes. (a) Crystal structure and (b) packing of **2-Ad-Pt-Cl**; (c) crystal structure and (d) packing of **2-Ad-Pt-CN**; (e) crystal structure, (f) straight packing, and (g) zigzag packing of **2-Ph-Pt-Cl**. For clarity, hydrogen atoms, crystallization solvent molecules, and PF₆⁻ anions are not shown. (a, c, e) Thermal ellipsoids are shown with 30% probability.

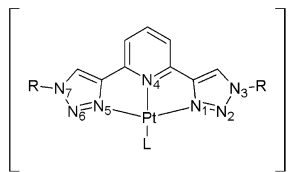
complexes were synthesized and purified by following adapted literature procedures^{37,69,39,40} in good to moderate yields (Scheme 1). The detailed synthetic procedures are described in the Experimental Section. (N[^]N[^]N)Pt(II)Cl complexes were prepared by refluxing a mixture of Pt(DMSO)₂Cl₂ and the

respective tridentate ligand (**2-Ad** or **2-Ph**) in dry MeOH under N₂ atmosphere for 48 h, followed by anionic exchange with aqueous solution of NH₄PF₆. Crystals of **2-Ad-Pt-Cl** were grown by slow diffusion of diethyl ether (Et₂O) into a solution of the complex in dichloromethane (DCM) at rt. The crystal

structure and packing are shown in Figure 1a,b, respectively. The shortest distance between two adjacent Pt(II) centers is 6.889 Å, which is too long to permit an electronic interaction between d_z^2 orbitals (typically 3.5 Å or shorter). The slow evaporation of an acetonitrile (ACN) solution of **2-Ad-Pt-CN** at rt gave crystals suitable for X-ray analysis. Figure 1c,d shows the crystal structure of **2-Ad-Pt-CN** and the corresponding packing. For this complex, we observed an alternating arrangement of the molecules with distances of 4.418 and 3.485 Å, thus minimizing the contact between the bulky adamantyl groups.

Crystals of **2-Ph-Pt-Cl** were obtained from a mixture of acetone and ACN (1:1) at rt. The crystal structure and packings are shown in Figure 1e–g. Replacement of the bulky adamantyl by the flat phenyl and keeping Cl^- as the ancillary ligand leads to two different packing modes within the crystal (straight and zigzag) for this complex. The straight packing has an arrangement of Pt centers at alternating distances of 3.445 and 3.424 Å. On the other hand, the zigzag packing showed an alternating organization of metal ions at distances of 3.487 and 3.407 Å. The selected crystal structure parameters of **2-Ad-Pt-Cl**, **2-Ph-Pt-Cl**, and **2-Ad-Pt-CN** are reported in Table 1.

Table 1. Selected Bond Lengths (Å) and Angles (deg) of the Complexes



R = Ad, Ph
L = Cl^- , CN^-

bond length (Å)	bond angle (deg)	2-Ad-Pt-Cl		2-Ph-Pt-Cl		2-Ad-Pt-CN	
		(Å)	(deg)	(Å)	(deg)	(Å)	(deg)
Pt–N1	N5–Pt–N4	1.996	80.17	1.960	81.7	1.981	79.5
Pt–N4	N1–Pt–N4	1.971	79.94	2.103	80.2	2.003	80.2
Pt–N5	N1–Pt–L	1.990	100.05	1.959	99.4	1.988	99.8
Pt–L	N5–Pt–L	2.277	99.84	2.302	98.7	1.974	100.6
	N5–Pt–N1		160.11		161.9		159.6
	N4–Pt–L		179.99		179.6		179.5

The absorption spectra of all the complexes in aerated ACN at rt are shown in Figure 2a. All the spectra show tridentate ligand-centered (^1LC) π – π^* transitions (300–340 nm), as well as the characteristic metal-to-ligand charge-transfer ($^1\text{MLCT}$) bands (350–390 nm). The extended conjugation provided by the phenyl moieties enhances the LC bands, whereas for $(\text{N}^{\wedge}\text{N}^{\wedge}\text{N})\text{Pt}(\text{II})\text{CN}$ complexes an additional feature is observed at 315 nm, which can be attributed to the presence of the electron-accepting CN^- ligand coordinated to the Pt(II) center, as already reported for similar compounds.^{69,70}

The complexes are nonluminescent in aerated and deaerated solutions at rt. Such lack of emission is most likely due to the thermal accessibility of MC excited states acting as nonradiative

deactivation channels. Furthermore, the $(\text{N}^{\wedge}\text{N}^{\wedge}\text{N})\text{Pt}(\text{II})\text{Cl}$ complexes do not show luminescence even in the solid state. Replacement of Cl^- by CN^- enables phosphorescence in solid state neat films (Figure 2b) and powders (Supporting Information, Figure S1). The CN^- ancillary ligand acts as a good π -acceptor and stabilizes the lowest occupied d-orbitals, which in turn hampers the thermal population of the MC states. In contrast, halides rather act as π -donors, destabilizing the occupied d-orbitals and consequently decreasing the energy gap of the MC states. Because of its π -accepting character, CN^- has an electron-withdrawing effect on the Pt(II) center, thus decreasing the electron density on the metal ion and favoring the interaction between the adjacent d_z^2 orbitals of two complexes, as can be observed by comparison of the crystal structures of **2-Ad-Pt-Cl** and **2-Ad-Pt-CN** (vide supra). Moreover, the metal–metal interactions trigger phosphorescence from the aggregated species. The emission and excitation spectra of $(\text{N}^{\wedge}\text{N}^{\wedge}\text{N})\text{Pt}(\text{II})\text{CN}$ complexes in neat films are shown in Figure 2b. Despite the bulky adamantyl groups, **2-Ad-Pt-CN** shows luminescence from a $^3\text{MMLCT}$ state (metal–metal-to-ligand charge transfer). Indeed, for this complex the shortest distance measured in the single crystal between the adjacent Pt(II) centers is 3.485 Å, which suggests metal–metal interactions (see Figure 1d). Stronger interactions are observed for complex **2-Ph-Pt-CN**, since the extended aromatic system of the phenyl groups also favors π – π interactions, which in turn triggers the Pt...Pt contacts. Indeed, **2-Ad-Pt-CN** emits at 560 nm, whereas **2-Ph-Pt-CN** shows a bathochromic shift of 10 nm (315 cm^{-1} , Figure 2b). Furthermore, the emission onset of **2-Ad-Pt-CN** occurs at ca. 475 nm, whereas for **2-Ph-Pt-CN**, it is observed at 510 nm. The stronger electronic coupling for the **2-Ph-Pt-CN** complex is also observed in the excitation profile in which the ground state aggregation is clearly seen as a band at 485 nm (Figure 2b). This $^1\text{MMLCT}$ band is absent in the absorption spectra in solution, confirming that the luminescence in the solid state is due to the aggregated form. The photophysical properties of powders of both $(\text{N}^{\wedge}\text{N}^{\wedge}\text{N})\text{Pt}(\text{II})\text{CN}$ complexes closely resemble the ones in the neat films (Figure S1 and Table 2). However, the emission maxima appear slightly blue-shifted, as compared to the neat films (10 nm, 325 cm^{-1} for **2-Ad-Pt-CN** and 5 nm, 155 cm^{-1} for **2-Ph-Pt-CN**). The emission and excitation profiles of both complexes in neat films and powders are independent of the excitation and emission wavelengths, respectively. The excited-state lifetimes of both $(\text{N}^{\wedge}\text{N}^{\wedge}\text{N})\text{Pt}(\text{II})\text{CN}$ complexes are biexponential in solid state. **2-Ad-Pt-CN** displays a longer lifetime and a lower photoluminescent quantum yield (PLQY), whereas **2-Ph-Pt-CN** shows shorter lifetimes and higher PLQY, pointing toward higher k_f and stronger Pt(II)–Pt(II) interactions compared to those of **2-Ad-Pt-CN**. Formation of the luminescent MMLCT state for **2-Ph-Pt-CN**, due to the assembly of several platinum units, leads to an emission quantum yield of 26% in neat films (Table 2), whereas **2-Ad-Pt-CN** shows only a modest emission in the solid state (PLQY = 0.4%).

In 2-MeTHF (THF = tetrahydrofuran) frozen matrices at 77 K, the emission spectrum of **2-Ad-Pt-CN** displays a structured vibrational progression peaking at 425, 450, and 485 nm, which can be assigned to the emission from the monomeric species (Figure 3a). However, the relative intensity of the emission maximum at 485 nm varies depending on the excitation wavelength. The relative intensity of the band at 485 nm increases as the excitation wavelength is shifted to the red. This

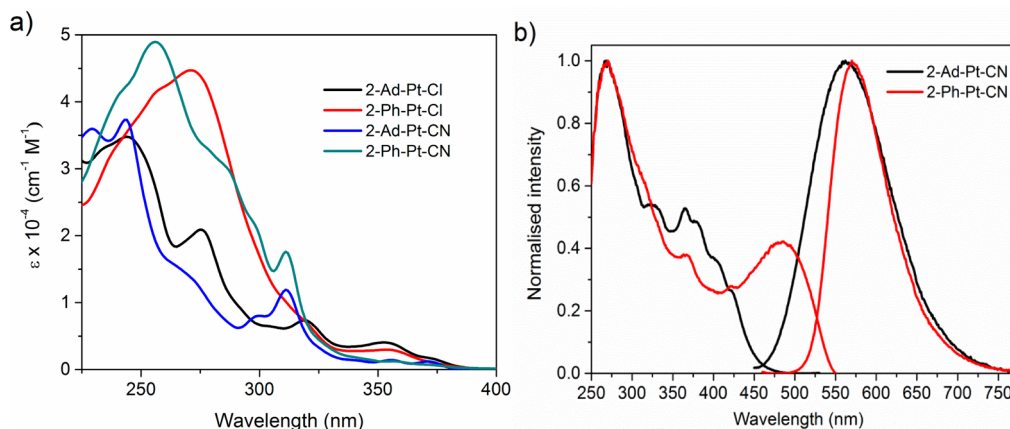


Figure 2. (a) Room temperature absorption spectra of $(N^N^N)Pt(II)Cl$ and $(N^N^N)Pt(II)CN$ complexes in aerated acetonitrile (1×10^{-5} M) and (b) emission and excitation spectra of $(N^N^N)Pt(II)CN$ complexes in neat film state. For the emission, $\lambda_{em} = 420$ nm, and for the excitation, $\lambda_{ex} = 565$ nm.

Table 2. Photophysical Properties of Pt(II) Complexes in Solid State at Room Temperature and at 77 K in 2-MeTHF

sample	$\lambda_{em}/\lambda_{ex}$ ^a (nm)	τ (μ s)	Φ ($\times 100$) ^b
2-Ad-Pt-CN, powder	550/431	1.62 (38%), 0.78 (62%)	0.4 ^c
2-Ad-Pt-CN, neat film	560/431	1.67 (66%), 0.58 (34%)	5.5 ^c
2-Ph-Pt-CN, powder	565/431	0.08 (57%), 0.20(43%)	16.5 ^d
2-Ph-Pt-CN, neat film	570/431	0.09 (78%), 0.24 (22%)	26 ^e
2-Ad-Pt-CN, 77 K	450/315	38.28	
2-Ad-Pt-CN, 77 K	485/315	37.82(45%), 3.55 (55%)	
2-Ph-Pt-CN, 77 K	445/365	1.89 (65%), 19.43 (35%)	
2-Ph-Pt-CN, 77 K	635/365	1.51 (92%), 9.26 (8%)	
2-Ad-Pt-Cl, 77 K	445/310	40.42	
2-Ad-Pt-Cl, 77 K	685/310	14.74	
2-Ph-Pt-Cl, 77 K	450/360	32.99	
2-Ph-Pt-Cl, 77 K	605/360	1.64 (71%), 10.99 (29%)	

^aExcitation and emission wavelengths used for monitoring the lifetimes. ^bQuantum yields measured with an integrating sphere. ^c $\lambda_{ex} = 425$ nm. ^d $\lambda_{ex} = 370$ nm. ^e $\lambda_{ex} = 420$ or 485 nm.

suggests that the emission of 2-Ad-Pt-CN has a fundamental contribution from the monomer and a weaker contribution

from interacting Pt(II) centers. This assignment is further supported by a weak new band in the excitation spectrum (at 395 nm) when the emission is monitored at 485 nm. The crystal structure previously suggested that metal–metal interactions (Figure 1d) can indeed be responsible for the aggregate emission. The excited state lifetime of the monomer (38 μ s, see Table 2) is longer than the one previously described for analogous bis-1,2,4-triazole or bis-tetrazole Pt(II) complexes (14 μ s for 1,2,4-triazoles and 13 μ s for tetrazoles).^{55,71} The extremely long excited-state lifetime suggests that the emitting state of the monomeric species is predominantly ligand-centered in nature, as also corroborated by the highly vibrationally structured emission. A biexponential lifetime is obtained when the emission is monitored at 485 nm, and we attributed this luminescence band to a mixture of the monomeric and the aggregated forms, where the latter are responsible for the shorter lifetime component (3.5 μ s). On the other hand, 2-Ph-Pt-CN displays a different behavior as the short Pt–Pt distance is indeed responsible for the stabilization of the aggregated species leading to an excitation wavelength-dependent emission. The coexistence of both forms, the monomeric and the aggregated species, is clearly seen upon excitation at shorter wavelength (365 nm). The complex indeed displays two distinct features: a weak structured emission with maxima at 420, 445, and 495 nm, and a strong unstructured

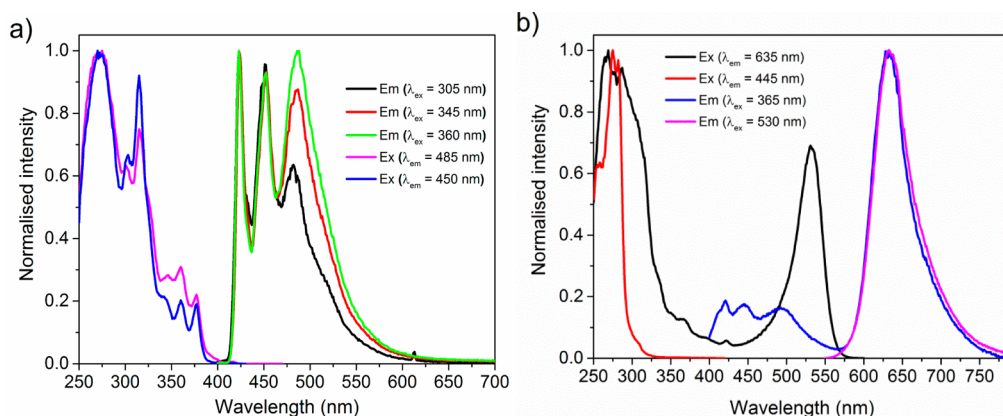


Figure 3. Emission and excitation spectra of $(N^N^N)Pt(II)CN$ complexes in 2-MeTHF glassy matrices at 77 K using different wavelengths, (a) 2-Ad-Pt-CN and (b) 2-Ph-Pt-CN.

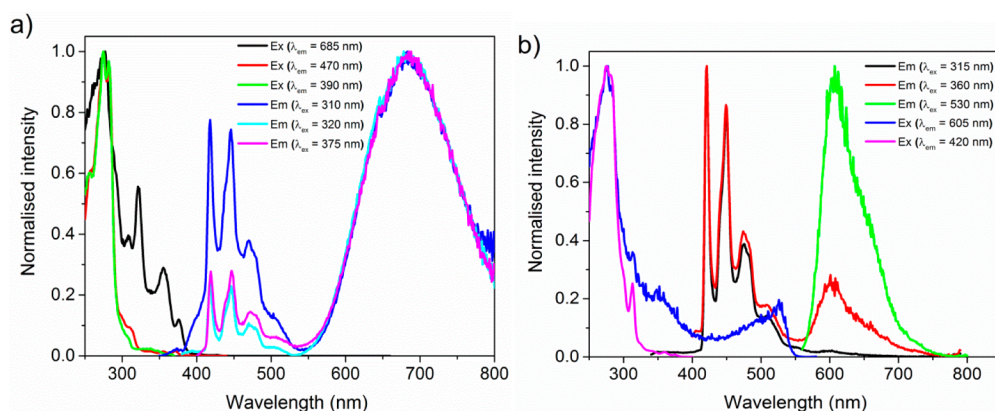


Figure 4. Emission and excitation spectra of (N^NN)Pt(II)Cl complexes in 2-MeTHF glassy matrices at 77 K at different wavelengths. (a) 2-Ad-Pt-Cl and (b) 2-Ph-Pt-Cl.

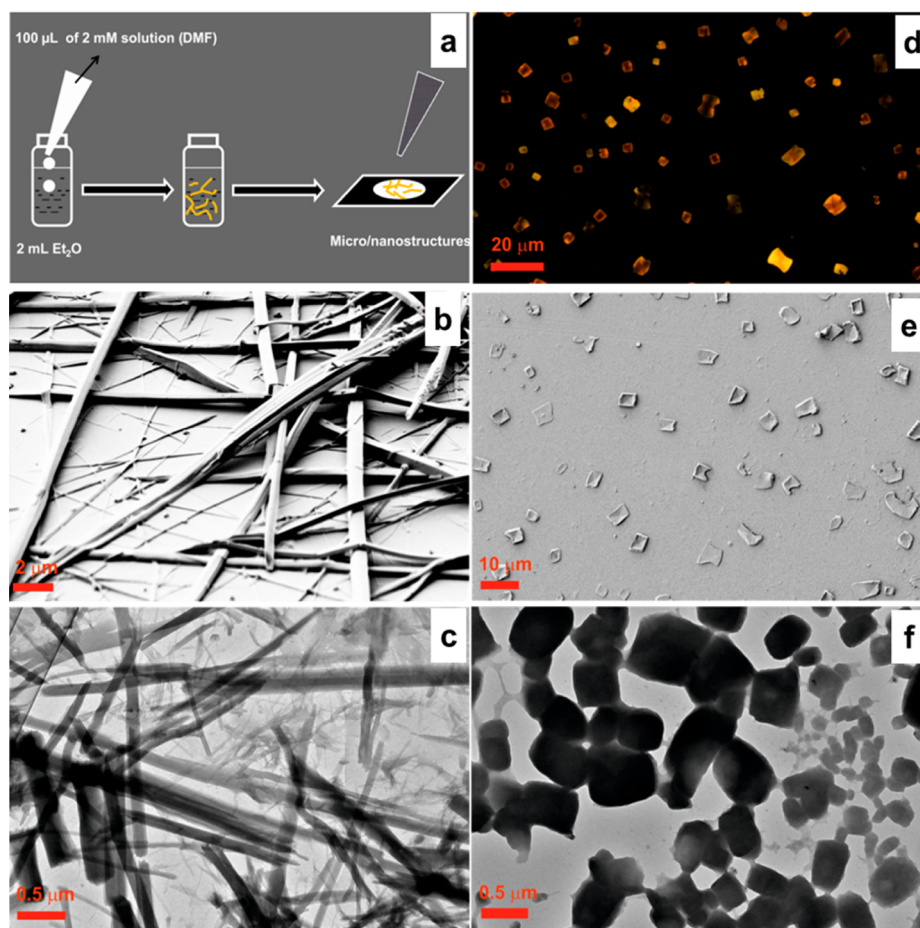


Figure 5. (a) Pictorial description of the preparation of self-assembled micro/nanostructures. (b) SEM and (c) TEM images of micro/nanostructures of 2-Ad-Pt-CN. (d) Optical fluorescence microscopy, (e) SEM and (f) TEM images of micro/nanostructures of 2-Ph-Pt-CN.

luminescence at 635 nm (Figure 3b). The structured emission can be assigned to the ³LC transitions of the monomer, whereas the unstructured profile is characteristic of the ³MMLCT decay of the aggregate. When the glassy matrix is excited at longer wavelength (530 nm), only the emission of the aggregate is observed (635 nm). This assignment is additionally supported by the excitation spectra. When the emission is monitored at 635 nm, the excitation profile shows an additional band at 530 nm, which can be assigned to the ¹MMLCT absorption. The different nature of the excited states

is also mirrored in the excited-state lifetimes, which are biexponential, and the longer component is assigned to the monomer and the shorter lived emission is assigned to the aggregate (Table 2). The relative weight of the lifetimes depends on the excitation wavelength and follows the emission behavior. Indeed, the longer lifetime has a relatively small weight when the emission is monitored at the emission maximum of the aggregate (at 635 nm, $\tau_1 = 1.5 \mu\text{s}$, 92%; $\tau_2 = 9.26 \mu\text{s}$, 8%).

At low temperature, the complexes possessing the Cl⁻ as ancillary ligand are also emissive. Figure 4 shows the emission

and excitation spectra of (N[^]N[^]N[^])Pt(II)Cl complexes in 2-MeTHF glassy matrices at 77 K. The structured emission profile of 2-Ad-Pt-Cl with maxima at 420, 445, and 470 nm can be attributed to the monomeric species, whereas the broad and unstructured band at 685 nm can be assigned to an excimer-like state (Figure 4a). Indeed, the excitation spectrum monitored in one of the vibrational bands of the high emission (e.g., at 470 nm) as well as that recorded at 690 nm show only ¹LC ($\pi-\pi^*$) and ¹MLCT absorption bands. These observations are consistent with the crystal structure, as there is no indication for ground-state Pt(II)–Pt(II) interactions (Figure 1b). The lifetime of the monomer of 2-Ad-Pt-Cl is on the order of 40 μ s, whereas the lifetime of the excimer, emitting in the deep red region, is \sim 15 μ s (see Table 2). The complex containing phenyls as substituents of the triazoles, 2-Ph-Pt-Cl, also shows a dual emission (Figure 4b), displaying structured bands at 420, 450, and 470 nm (monomeric species) and a broad luminescence at 605 nm (aggregated species). The excitation spectra monitored on the high-energy emission consist of typical ¹LC (300–340 nm) and ¹MLCT (360–400 nm) absorption bands. On the other hand the excitation spectrum obtained for the low energy (605 nm), displays a new band at 530 nm, along with ¹LC and ¹MLCT bands. Such observations indicate that the red emission is generated by an aggregate formed already in the ground state. The crystal structure indeed confirms the strong electronic interactions between the platinum units (Figure 1f,g) in the solid state. The decay of the monomer emission is monoexponential (33 μ s, see Table 2), whereas a biexponential decay is observed when emission is monitored at the emission maximum of the aggregate (1.64 μ s (71%) and 11 μ s (29%), see Table 2), which points toward different types of aggregates with different rigidity.

To understand if the morphology and size of the aggregates are the same for (N[^]N[^]N[^])Pt(II)CN complexes, the assembled structures were investigated using an identical preparation strategy for both complexes, as shown in the schematic diagram of Figure 5a. The assemblies were obtained by following reprecipitation method, dropping 100 μ L of a dimethylformamide (DMF) solution of the complex (2 mM) into 2 mL of Et₂O.⁶¹ As soon as the DMF solution is added to Et₂O, a turbid suspension is formed. The resulting suspension was analyzed by electron and optical microscopies. The morphology of the self-assembled micro/nanostructures of 2-Ad-Pt-CN can be observed in the scanning electron microscopy (SEM) and transmission electron microscopy (TEM) images, showing tapelike and rodlike structures (Figure 5b,c). The width of these species is on the order of 100–500 nm, whereas the length reaches hundreds of micrometers. They did not show any detectable photoluminescence under the fluorescence microscope. Interestingly, the substitution pattern on the tridentate ligand has a clear influence on the morphology of the self-assembled micro/nanostructures, which is evidenced by complex 2-Ph-Pt-CN forming square platelets.

We observed that the microstructures are formed as soon as the DMF solution of 2-Ph-Pt-CN is dropped into Et₂O, and the assembly process can be followed by UV irradiation of the resulting photoluminescent suspension. In this case, the intrinsic luminescence of the assemblies enabled the characterization by optical fluorescence microscopy. Fluorescence microscopy and SEM and TEM images revealed square-shaped structures with characteristic dimensions of 2 μ m (Figure 5d–f). The selected area electron diffraction (SAED) measurements revealed the lack of crystallinity of these structures of

(N[^]N[^]N[^])Pt(II)CN complexes. To assess the effect of the ancillary ligand on the self-assembly process, micro/nano structures of the (N[^]N[^]N[^])Pt(II)Cl complexes were also prepared. Only a minor influence is observed on the morphology of 2-Ad-Pt-Cl (Figure S2), as compared to that of 2-Ad-Pt-CN, whereas the morphology of 2-Ph-Pt-Cl gave no defined structures.

CONCLUSIONS

We have synthesized a new series of tridentate ligands able to yield monocationic Pt(II) complexes. Two different substitution patterns (bulky adamantyl or planar phenyl) and two monoanionic ancillary ligands (Cl[−] and CN[−]) were chosen to investigate the effect of the structural variation on the photophysical properties. The (N[^]N[^]N[^])Pt(II)Cl complexes are nonluminescent at rt: 2-Ad-Pt-Cl bearing the two bulky adamantyl groups shows no Pt(II)–Pt(II) interactions, whereas for 2-Ph-Pt-Cl, the planar extended tridentate ligand assists the coupling of neighboring metal complexes. On the other hand, (N[^]N[^]N[^])Pt(II)CN complexes are luminescent both as powders and as neat films. Interestingly, the π -accepting nature of CN[−] induces Pt(II)–Pt(II) interactions irrespectively of bulky substitution patterns. The emission of 2-Ph-Pt-CN is red-shifted as compared to that of 2-Ad-Pt-CN, due to the planarity of the phenyl moieties. The highest quantum yield is attained with 2-Ph-Pt-CN in neat film (26%). 2-Ad-Pt-CN self-assembles into nonluminescent tapelike or rodlike structures, whereas 2-Ph-Pt-CN yields luminescent square-shaped platelets.

EXPERIMENTAL SECTION

Details regarding reagents, instrumentation, and X-ray crystal analysis are provided in the Supporting Information.

Synthesis of 2,6-Diethynylpyridine (1). 2,6-Dibromopyridine (2.368 g, 10 mmol), Pd(PPh₃)₄ (351 mg, 5% mmol), and NEt₃ (8 mL) were dissolved in toluene under N₂ atmosphere. To this mixture, CuI (190 mg, 10% mmol) and trimethylsilylacetylene (2.940 g, 30 mmol) were added, and the reaction mixture was heated to 35–40 °C overnight. The solvent was removed using a rotary evaporator. Using aqueous ammonia solution (32%), extraction was done with DCM to remove copper salts. Solvent was removed, and the product was redissolved in a mixture of MeOH and water (1:1) in the presence of KOH. This mixture was left stirring at rt overnight. The product was extracted into DCM (2 \times 150 mL). Organic fractions were combined and washed with brine and dried over MgSO₄. Solvent was removed under vacuum, and the crude product was purified by column chromatography (silica gel, 10% EtOAc in hexane). Yield: 63% (800 mg). ¹H NMR (300 MHz, CDCl₃): δ 7.69–7.57 (m, 1H), 7.42 (d, J = 7.8 Hz, 2H), 3.14 (s, 2H). ¹³C NMR (75 MHz, CDCl₃): δ 142.76 (s), 136.66 (s), 127.19 (s), 82.14 (s), 77.87 (s). High-resolution mass spectrometry (HRMS) electrospray ionization (ESI) m/z : Calculated, 150.0319 [M + Na]⁺; found, 150.0310 [M + Na]⁺, 128.0491 [M + H]⁺.

Synthesis of 2,6-Bis(3-(adamantan-1-yl)-1H-1,2,3-triazol-5-yl)pyridine (2-Ad). A mixture of compound 1 (127 mg, 1 mmol), 1-azidoadamantane (444 mg, 2.5 mmol), and dry THF was bubbled with N₂ gas. CuBr (57.4 mg, 0.4 mmol) and N,N,N',N',N''-pentamethyldiethylenetriamine (85.2 μ L, 0.4 mmol) were dissolved separately in dry THF in another round-bottom flask. These mixtures were added together and stirred under N₂ for 24 h. An aqueous ammonia solution (32%) was added to the reaction mixture and stirred for 2 h. THF was removed under vacuum. Extraction was done between DCM and water to remove the copper salts. The organic fractions were combined and washed with brine and dried over MgSO₄ followed by removal of solvent using a rotary evaporator. The crude was further purified by column chromatography (silica gel, 30% EtOAc

in hexane). Yield: 72.3% (348 mg). ^1H NMR (300 MHz, CD_2Cl_2): δ 8.56 (s, 2H), 8.12 (d, $J = 7.9$ Hz, 2H), 7.96–7.88 (m, 1H), 2.12 (dd, $J = 53.0$, 26.6 Hz, 18H), 1.79–1.60 (m, 12H). ^{13}C NMR (75 MHz, CD_2Cl_2): δ 151.38 (s), 147.64 (s), 138.63 (s), 119.47 (d, $J = 61.7$ Hz), 60.20 (s), 43.19 (s), 36.26 (s), 30.05 (s). HRMS (ESI) m/z : Calculated, 504.2851 $[\text{M} + \text{Na}]^+$; found, 504.2845 $[\text{M} + \text{Na}]^+$. X-ray crystal structure analysis: formula $\text{C}_{29}\text{H}_{35}\text{N}_7$, $M = 481.64$, yellow crystal, $0.30 \times 0.23 \times 0.20$ mm, $a = 18.8888(4)$, $b = 11.6902(2)$, $c = 11.2906(2)$ Å, $\beta = 96.767(1)^\circ$, $V = 2475.75(8)$ Å³, $\rho_{\text{calc}} = 1.292$ g cm⁻³, $\mu = 0.080$ mm⁻¹, empirical absorption correction ($0.976 \leq T \leq 0.984$), $Z = 4$, monoclinic, space group $P2_1/c$ (No. 14), $\lambda = 0.71073$ Å, $T = 223(2)$ K, ω and φ scans, 16 558 reflections collected ($\pm h$, $\pm k$, $\pm l$), $[(\sin \theta)/\lambda] = 0.60$ Å⁻¹, 5779 independent ($R_{\text{int}} = 0.048$) and 4410 observed reflections [$I > 2\sigma(I)$], 353 refined parameters, $R = 0.071$, $wR^2 = 0.167$, max (min) residual electron density 0.29 (-0.25) e·Å⁻³, hydrogen atoms calculated and refined as riding atoms.

Synthesis of Phenylazide. Phenylazide was synthesized by following a literature report.⁷² Aniline (1.567 mL, 17.2 mmol) was dissolved in ACN and cooled to 0 °C. To this mixture, *t*-BuNO₂ (3 mL, 25.6 mmol) was added followed by dropwise addition of trimethylsilyl azide (2.72 mL, 20.4 mmol). The reaction mixture was left stirring at rt for 2.5 h. The reaction mixture was concentrated under reduced pressure, and the product was purified by column chromatography (silica gel, hexane). The product constituted a yellow oil. Yield: 75% (1530 mg). ^1H NMR (300 MHz, CDCl_3): δ 7.41–7.33 (m, 1H), 7.19–7.11 (m, 1H), 7.04 (ddd, $J = 2.8$, 2.3, 1.1 Hz, 1H).

Synthesis of 2,6-Bis(3-phenyl-1H-1,2,3-triazol-5-yl)pyridine (2-Ph). In a 100 mL round-bottom flask, compound **1** (204 mg, 1.6 mmol) and phenylazide (400 mg, 3.36 mmol) were dissolved in a mixture of *t*-BuOH/water (1:1) (16 mL) under N₂. Sodium ascorbate (158 mg, 0.8 mmol) and CuSO₄·5H₂O (80 mg, 0.32 mmol) were added, and the reaction mixture was stirred at rt under N₂ for 24 h. To get rid of the copper salts, an aqueous ammonia solution was added to reaction mixture and stirred for 1 h. The product was then extracted into DCM. The organic layer was washed with brine and dried over MgSO₄ followed by removal of the solvent using a rotary evaporator. The crude mixture was purified by column chromatography (silica gel, 50% EtOAc in hexane). Yield: 80% (467 mg). ^1H NMR (300 MHz, CDCl_3): δ 8.73 (s, 2H), 8.26–8.17 (m, 2H), 7.99–7.90 (m, 1H), 7.87–7.77 (m, 4H), 7.59–7.50 (m, 4H), 7.50–7.41 (m, 2H). ^{13}C NMR (75 MHz, CDCl_3): δ 149.77 (s), 148.70 (s), 138.25 (s), 137.06 (s), 129.93 (s), 129.07 (s), 120.54 (d, $J = 13.0$ Hz), 119.98 (s). HRMS (ESI) m/z : Calculated, 388.1286 $[\text{M} + \text{Na}]^+$; found, 388.1281 $[\text{M} + \text{Na}]^+$, 366.1452 $[\text{M} + \text{H}]^+$.

Synthesis of Pt(DMSO)₂Cl₂. K₂PtCl₄ (5 g, 1 equiv) and DMSO (2.6 mL, 3 equiv) were dissolved in 50 mL of water in a one necked round-bottom flask. This reaction mixture was stirred at rt for 4 h. During this period, an ash-colored precipitate was formed, which was removed by filtration, washed with water, and then washed with Et₂O. The product was dried under vacuum before further usage. Yield: 84.2% (4.283 g).

Synthesis of 2-Ad-Pt-Cl. 2-Ad (505 mg, 1.05 mmol) and Pt(DMSO)₂Cl₂ (422 mg, 1 mmol) were dissolved in dry MeOH and refluxed under N₂ for 48 h. After 1 h of reflux, a yellow precipitate formed. After it cooled to rt, the yellow precipitate was filtered and washed with Et₂O to remove traces of unreacted 2-Ad. Then the crude product was redissolved in a minimum amount of DMSO by gentle heating. An aqueous solution of NH₄PF₆ was added (dropwise), and a precipitate formed, which was filtered off and washed with water to remove the excess of NH₄PF₆. The precipitate was further washed with Et₂O, and the crude product was purified by column chromatography (silica gel, 5–10% MeOH in DCM). Yield: 75% (642 mg). ^1H NMR (300 MHz, DMSO-*d*₆): δ 9.48 (s, 2H), 8.40 (t, $J = 8.0$ Hz, 1H), 7.98 (d, $J = 8.0$ Hz, 2H), 2.23 (s, 18H), 1.72 (s, 12H). ^{13}C NMR (75 MHz, DMSO-*d*₆): δ 150.17 (s), 147.76 (s), 143.32 (s), 125.66 (s), 120.37 (s), 64.16 (s), 41.64 (s), 34.93 (s), 29.00 (s). ^{19}F NMR (282 MHz, DMSO-*d*₆): δ -68.87 (s), -71.39 (s). HRMS (ESI) m/z : Calculated, 712.2283 $[\text{M}]^+$; found, 712.2280 $[\text{M}]^+$, 707.2790 $[\text{M} - \text{Cl} + \text{OCH}_3]^+$. CHN Analysis: Calculated (C₂₉H₃₅ClN₇PF₆Pt), C, 40.64%; H, 4.12%; N, 11.44%; found, C, 40.80%; H, 4.16%; N, 11.14%. X-ray crystal

structure analysis: formula C₂₉H₃₅ClN₇PF₆Pt·C₄H₁₀O·2 × CH₂Cl₂, $M = 1101.12$, yellow crystal, $0.40 \times 0.07 \times 0.07$ mm, $a = 17.3619(2)$, $b = 6.8895(1)$, $c = 18.4882(3)$ Å, $\beta = 102.457(1)^\circ$, $V = 2159.40(5)$ Å³, $\rho_{\text{calc}} = 1.693$ g cm⁻³, $\mu = 3.660$ mm⁻¹, empirical absorption correction ($0.322 \leq T \leq 0.783$), $Z = 2$, monoclinic, space group $P2_1/m$ (No. 11), $\lambda = 0.71073$ Å, $T = 223(2)$ K, ω and φ scans, 13 947 reflections collected ($\pm h$, $\pm k$, $\pm l$), $[(\sin \theta)/\lambda] = 0.66$ Å⁻¹, 4082 independent ($R_{\text{int}} = 0.033$) and 3977 observed reflections [$I > 2\sigma(I)$], 316 refined parameters, $R = 0.026$, $wR^2 = 0.069$, max (min) residual electron density 1.34 (-0.78) e·Å⁻³, hydrogen atoms calculated and refined as riding atoms.

Synthesis of 2-Ph-Pt-Cl. 2-Ph (383 mg, 1.05 mmol) and Pt(DMSO)₂Cl₂ (422 mg, 1 mmol) were dissolved in dry MeOH and refluxed under N₂ atmosphere for 48 h. After 1 h of reflux, a yellow precipitate formed. After it cooled to rt, the yellow precipitate was filtered and washed with Et₂O to remove traces of unreacted 2-Ph. Then the crude product was redissolved in a minimum amount of DMSO by gentle heating. An aqueous solution of NH₄PF₆ was added (dropwise), and a precipitate formed, which was filtered off and washed with water to remove the excess of NH₄PF₆. The crude was purified by column chromatography (neutral Al₂O₃, 10–15% MeOH in DCM). Yield: 80% (505 mg). ^1H NMR (300 MHz, DMSO-*d*₆): δ 9.38 (s, 2H), 8.11–8.05 (m, 2H), 8.05–7.98 (m, 1H), 7.71–7.61 (m, 4H), 7.59–7.50 (m, 4H), 7.45–7.34 (m, 2H). ^{13}C NMR (75 MHz, DMSO-*d*₆): δ 149.46 (s), 148.18 (s), 138.68 (s), 136.58 (s), 130.04 (s), 129.10 (s), 121.94 (s), 120.39 (s), 118.86 (s). HRMS (ESI) m/z : Calculated, 596.0711 $[\text{M}]^+$; found, 596.0688 $[\text{M}]^+$, 591.1203 $[\text{M} - \text{Cl} + \text{OCH}_3]^+$. CHN Analysis: Calculated (C₂₁H₁₅ClN₇PF₆Pt), C, 39.95%; H, 2.39%; N, 15.53%; found, C, 39.67%; H, 2.54%; N, 15.19%. X-ray crystal structure analysis: formula C₂₁H₁₅ClN₇PF₆Pt, $M = 740.91$, yellow crystal, $0.12 \times 0.06 \times 0.02$ mm, $a = 6.8613(2)$, $b = 17.8733(4)$, $c = 20.9936(4)$ Å, $\alpha = 72.697(1)$, $\beta = 87.112(1)$, $\gamma = 83.748(1)^\circ$, $V = 2442.9(1)$ Å³, $\rho_{\text{calc}} = 2.014$ g cm⁻³, $\mu = 5.990$ mm⁻¹, empirical absorption correction ($0.533 \leq T \leq 0.889$), $Z = 4$, triclinic, space group $P\bar{1}$ (No. 2), $\lambda = 0.71073$ Å, $T = 223(2)$ K, ω and φ scans, 20 859 reflections collected ($\pm h$, $\pm k$, $\pm l$), $[(\sin \theta)/\lambda] = 0.59$ Å⁻¹, 8390 independent ($R_{\text{int}} = 0.039$) and 7478 observed reflections [$I > 2\sigma(I)$], 667 refined parameters, $R = 0.069$, $wR^2 = 0.192$, max (min) residual electron density 1.88 (-1.88) e·Å⁻³, hydrogen atoms calculated and refined as riding atoms.

Synthesis of 2-Ad-Pt-CN. A mixture of 2-Ad-Pt-Cl (85.7 mg, 0.1 mmol) and AgCN (24 mg, 0.18 mmol) in ACN was heated at 65 °C for 4 h under N₂ atmosphere. The hot reaction mixture was filtered through a pad of Celite. The filtrate was concentrated under vacuum and further purified by column chromatography (silica gel, 5% MeOH in DCM). Yield: 65% (55.1 mg). ^1H NMR (300 MHz, CD_2Cl_2): δ 8.66 (s, 2H), 8.23 (dd, $J = 8.5$, 7.6 Hz, 1H), 8.02 (d, $J = 7.9$ Hz, 2H), 2.36 (s, 18H), 1.84 (s, 12H). ^{13}C NMR (75 MHz, CD_2Cl_2): δ 151.13 (s), 148.70 (s), 144.62 (s), 124.92 (s), 121.34 (s), 66.29 (s), 42.79 (s), 35.81 (s), 30.21 (s). ^{19}F NMR (282 MHz, CD_2Cl_2): δ -70.40 (d, $J = 1.0$ Hz), -72.92 (d, $J = 1.0$ Hz). HRMS (ESI) m/z : Calculated, 702.2629 $[\text{M}]^+$; found, 702.2621 $[\text{M}]^+$. CHN Analysis: Calculated (C₃₀H₃₅N₈PF₆Pt+MeOH), C, 42.32%; H, 4.47%; N, 12.74%; found, C, 42.19%; H, 4.47%; N, 12.45%. X-ray crystal structure analysis: formula C₃₀H₃₅N₈PF₆Pt·3 × C₂H₃N, $M = 970.88$, yellow crystal, $0.50 \times 0.07 \times 0.01$ mm, $a = 19.6031(4)$, $b = 13.6843(3)$, $c = 29.6267(6)$ Å, $\beta = 95.421(1)^\circ$, $V = 7912.0(3)$ Å³, $\rho_{\text{calc}} = 1.630$ g cm⁻³, $\mu = 3.658$ mm⁻¹, empirical absorption correction ($0.262 \leq T \leq 0.964$), $Z = 8$, monoclinic, space group $P2_1/n$ (No. 14), $\lambda = 0.71073$ Å, $T = 223(2)$ K, ω and φ scans, 54 298 reflections collected ($\pm h$, $\pm k$, $\pm l$), $[(\sin \theta)/\lambda] = 0.59$ Å⁻¹, 13 670 independent ($R_{\text{int}} = 0.088$) and 11 062 observed reflections [$I > 2\sigma(I)$], 997 refined parameters, $R = 0.066$, $wR^2 = 0.142$, max (min) residual electron density 1.28 (-1.30) e·Å⁻³, hydrogen atoms calculated and refined as riding atoms.

Synthesis of 2-Ph-Pt-CN. A mixture of 2-Ph-Pt-Cl (74 mg, 0.1 mmol) and AgCN (24 mg, 0.18 mmol) in ACN was heated at 65 °C for 4 h under N₂ atmosphere. The hot reaction mixture was filtered through a pad of Celite to remove the precipitated silver chloride. The filtrate was concentrated under vacuum and further purified by column chromatography (neutral Al₂O₃, 5–10% MeOH in DCM). Yield: 62%

(45.3 mg). ^1H NMR (300 MHz, $\text{DMF-}d_7$): δ 10.15 (s, 2H), 8.76 (dd, J = 8.4, 7.7 Hz, 1H), 8.50 (d, J = 8.0 Hz, 2H), 8.14–8.05 (m, 4H), 7.90–7.74 (m, 6H). ^{13}C NMR (75 MHz, $\text{DMF-}d_7$): δ 153.76 (s), 149.00 (s), 146.36 (s), 136.99 (s), 132.36 (s), 131.57 (s), 128.49–127.78 (m), 122.78 (s), 122.47 (s). ^{19}F NMR (282 MHz, $\text{DMF-}d_7$): δ –70.59 (s), –73.10 (s). HRMS (ESI) m/z : Calculated, 586.1063 $[\text{M}]^+$; found, 586.1062 $[\text{M}]^+$.

■ ASSOCIATED CONTENT

● Supporting Information

Materials, instrumentation, methods of X-ray diffraction analysis, tabulated bond lengths and angles of **2-Ad**, **2-Ad-Pt-Cl**, **2-Ph-Pt-Cl**, and **2-Ad-Pt-CN**, emission and excitation spectra, and SEM images. This material is available free of charge via the Internet at <http://pubs.acs.org>.

■ AUTHOR INFORMATION

Corresponding Authors

*E-mail: ca.s@wwu.de.

*E-mail: decola@unistra.fr.

Present Addresses

¹Institut für Organische Chemie, Universität Würzburg, Am Hubland, 97074 Würzburg, Germany.

^{II}Institut de Science et d'Ingénierie Supramoléculaires, Université de Strasbourg, 8 Rue Gaspard Monge, 67000 Strasbourg, France.

Notes

The authors declare no competing financial interest.

■ ACKNOWLEDGMENTS

N. K. A. acknowledges the NRW Graduate School of Chemistry (NRW GSC-MS) for doctoral fellowship. We acknowledge Dr. H. Lülff for the SEM images.

■ REFERENCES

- Turner, E.; Bakken, N.; Li, J. *Inorg. Chem.* **2013**, *52*, 7344–7351.
- Yersin, H. *Highly Efficient OLEDs with Phosphorescent Materials*; Wiley-VCH Verlag GmbH & Co. KGaA: Weinheim, Germany, 2008.
- Müllen, K. *Organic Light-Emitting Devices: Synthesis, Properties and Applications*; Wiley-VCH Verlag GmbH & Co. KGaA: Weinheim, Germany, 2006.
- Kalinowski, J.; Fattori, V.; Cocchi, M.; Williams, J. A. G. *Coord. Chem. Rev.* **2011**, *255*, 2401–2425.
- Chou, P.-T.; Chi, Y.; Chung, M.-W.; Lin, C.-C. *Coord. Chem. Rev.* **2011**, *255*, 2653–2665.
- Williams, J. A. G.; Develay, S.; Rochester, D.; Murphy, L. *Coord. Chem. Rev.* **2008**, *252*, 2596–2611.
- Xu, H.; Chen, R.; Sun, Q.; Lai, W.; Su, Q.; Huang, W.; Liu, X. *Chem. Soc. Rev.* **2014**, *43*, 3259–3302.
- Hua, F.; Kinayyigit, S.; Cable, J. R.; Castellano, F. N. *Inorg. Chem.* **2006**, *45*, 4304–4306.
- Rachford, A. A.; Hua, F.; Adams, C. J.; Castellano, F. N. *Dalton Trans.* **2009**, 3950–3954.
- Boixel, J.; Guerchais, V.; Le Bozec, H.; Jacquemin, D.; Amar, A.; Boucekkine, A.; Colombo, A.; Dragonetti, C.; Marinotto, D.; Roberto, D.; Righetto, S.; De Angelis, R. *J. Am. Chem. Soc.* **2014**, *136*, 5367–5375.
- Wadas, T. J.; Wang, Q. M.; Kim, Y. J.; Flaschenreim, C.; Blanton, T. N.; Eisenberg, R. *J. Am. Chem. Soc.* **2004**, *126*, 16841–16849.
- Kobayashi, A.; Yonemura, T.; Kato, M. *Eur. J. Inorg. Chem.* **2010**, *2010*, 2465–2470.
- Wong, K.; Yam, V. W. *Coord. Chem. Rev.* **2007**, *251*, 2477–2488.
- Ohba, T.; Kobayashi, A.; Chang, H.-C.; Kato, M. *Dalton Trans.* **2013**, *42*, 5514–5523.
- Zhao, Q.; Li, F.; Huang, C. *Chem. Soc. Rev.* **2010**, *39*, 3007–3030.
- Kobayashi, A.; Kato, M. *Eur. J. Inorg. Chem.* **2014**, *2014*, 4469–4483.
- Ma, D.-L.; Ma, V.; Chan, D.; Leung, K.-H.; He, H.-Z.; Leung, C.-H. *Coord. Chem. Rev.* **2012**, *256*, 3087–3113.
- Barton, J. K.; Olmon, E. D.; Sontz, P. A. *Coord. Chem. Rev.* **2011**, *255*, 619–634.
- Liu, H. K.; Sadler, P. J. *Acc. Chem. Res.* **2011**, *44*, 349–359.
- Cummings, S. D. *Coord. Chem. Rev.* **2009**, *253*, 1495–1516.
- Eryazici, I.; Moorefield, C. N.; Newkome, G. R. *Chem. Rev.* **2008**, *108*, 1834–1895.
- Howe-Grant, M.; Wu, K. C.; Bauer, W. R.; Lippard, S. J. *Biochemistry* **1976**, *15*, 4339–4346.
- Arena, G.; Scolaro, L. M.; Pasternack, R. F.; Romeo, R. *Inorg. Chem.* **1995**, *34*, 2994–3002.
- Natile, G.; Coluccia, M. *Coord. Chem. Rev.* **2001**, *216*–217, 383–410.
- Marzilli, L. G.; Ano, S. O.; Intini, F. P.; Natile, G. *J. Am. Chem. Soc.* **1999**, *121*, 9133–9142.
- Wang, D.; Lippard, S. J. *Nat. Rev. Drug Discovery* **2005**, *4*, 307–320.
- Lowe, G.; Droz, A. S.; Vilaivan, T.; Weaver, G. W.; Park, J. J.; Pratt, J. M.; Tweedale, L.; Kelland, L. R. *J. Med. Chem.* **1999**, *42*, 3167–3174.
- Kelland, L. *Nat. Rev. Cancer* **2007**, *7*, 573–584.
- Lippard, S. In *Platinum, Gold, and Other Metal Chemotherapeutic Agents*; ACS Symposium Series 209; American Chemical Society: Washington, DC, 1983.
- Wilson, J. J.; Lippard, S. J. *Chem. Rev.* **2014**, *114*, 4470–4495.
- Krause-Heuer, A. M.; Grunert, R.; Kuhne, S.; Buczkowska, M.; Wheate, N. J.; Le Pevelen, D. D.; Boag, L. R.; Fisher, D. M.; Kasparkova, J.; Malina, J.; Bednarski, P. J.; Brabec, V.; Aldrich-Wright, J. R. *J. Med. Chem.* **2009**, *52*, 5474–5484.
- Botchway, S. W.; Charnley, M.; Haycock, J. W.; Parker, A. W.; Rochester, D. L.; Weinstein, J. A.; Williams, J. A. G. *Proc. Natl. Acad. Sci. U. S. A.* **2008**, *105*, 16071–16076.
- Baggaley, E.; Botchway, S. W.; Haycock, J. W.; Morris, H.; Sazanovich, I. V.; Williams, J. A. G.; Weinstein, J. A. *Chem. Sci.* **2014**, *5*, 879–886.
- Zhao, Q.; Huang, C.; Li, F. *Chem. Soc. Rev.* **2011**, *40*, 2508–2524.
- Puntoriero, F.; Campagna, S.; Di Pietro, M. L.; Giannetto, A.; Cusumano, M. *Photochem. Photobiol. Sci.* **2007**, *6*, 357–360.
- Mauro, M.; Aliprandi, A.; Septiadi, D.; Kehr, N. S.; De Cola, L. *Chem. Soc. Rev.* **2014**, *43*, 4144–4166.
- Septiadi, D.; Aliprandi, A.; Mauro, M.; De Cola, L. *RSC Adv.* **2014**, *4*, 25709–25718.
- Ting, V. P.; Schmidtman, M.; Wilson, C. C.; Weller, M. T. *Angew. Chem., Int. Ed.* **2010**, *49*, 9408–9411.
- Flechon, A.; Culine, S.; Droz, J. P. *Crit. Rev. Oncol. Hematol.* **2001**, *37*, 35–46.
- Wheate, N. J.; Walker, S.; Craig, G. E.; Oun, R. *Dalton Trans.* **2010**, *39*, 8113–8127.
- Harper, B. W.; Krause-Heuer, A. M.; Grant, M. P.; Manohar, M.; Garbutcheon-Singh, K. B.; Aldrich-Wright, J. R. *Chem.—Eur. J.* **2010**, *16*, 7064–7077.
- Hall, M. D.; Okabe, M.; Shen, D. W.; Liang, X. J.; Gottesman, M. M. *Annu. Rev. Pharmacol. Toxicol.* **2008**, *48*, 495–535.
- Dhar, S.; Daniel, W. L.; Giljohann, D. A.; Mirkin, C. A.; Lippard, S. J. *J. Am. Chem. Soc.* **2009**, *131*, 14652–14653.
- Schilter, D.; Urathamakul, T.; Beck, J. L.; Harding, M. M.; Rendina, L. M. *Dalton Trans.* **2010**, *39*, 11263–11271.
- Wang, P.; Leung, C. H.; Ma, D. L.; Sun, R. W.; Yan, S. C.; Chen, Q. S.; Che, C. M. *Angew. Chem., Int. Ed.* **2011**, *50*, 2554–2558.
- Suntharalingam, K.; White, A. J.; Vilar, R. *Inorg. Chem.* **2010**, *49*, 8371–8380.

- (47) Suntharalingam, K.; White, A. J.; Vilar, R. *Inorg. Chem.* **2009**, *48*, 9427–9435.
- (48) Bertrand, H.; Bombard, S.; Monchaud, D.; Talbot, E.; Guedin, A.; Mergny, J. L.; Grunert, R.; Bednarski, P. J.; Teulade-Fichou, M. P. *Org. Biomol. Chem.* **2009**, *7*, 2864–2871.
- (49) Yu, C.; Chan, K. H.; Wong, K. M.; Yam, V. W. *Chem. Commun.* **2009**, 3756–3758.
- (50) Zhao, L.; Wong, K. M.; Li, B.; Li, W.; Zhu, N.; Wu, L.; Yam, V. W. *Chem.—Eur. J.* **2010**, *16*, 6797–6809.
- (51) Wong, K. M.; Yam, V. W. *Acc. Chem. Res.* **2011**, *44*, 424–434.
- (52) Strassert, C. A.; Chien, C. H.; Galvez Lopez, M. D.; Kourkoulos, D.; Hertel, D.; Meerholz, K.; De Cola, L. *Angew. Chem., Int. Ed.* **2011**, *50*, 946–50.
- (53) Mauro, M.; Aliprandi, A.; Cebrian, C.; Wang, D.; Kubel, C.; De Cola, L. *Chem. Commun.* **2014**, *50*, 7269–7272.
- (54) Allampally, N. K.; Bredol, M.; Strassert, C. A.; De Cola, L. *Chem.—Eur. J.* **2014**, *20*, 16863–16868.
- (55) Allampally, N. K.; Strassert, C. A.; De Cola, L. *Dalton trans.* **2012**, *41*, 13132–13137.
- (56) Krikorian, M.; Liu, S.; Swager, T. M. *J. Am. Chem. Soc.* **2014**, *136*, 2952–2955.
- (57) Kozhevnikov, V. N.; Donnio, B.; Bruce, D. W. *Angew. Chem., Int. Ed.* **2008**, *47*, 6286–6289.
- (58) Camerel, F.; Ziessel, R.; Donnio, B.; Bourgogne, C.; Guillon, D.; Schmutz, M.; Iacovita, C.; Bucher, J. P. *Angew. Chem., Int. Ed.* **2007**, *46*, 2659–2662.
- (59) Venkatesan, K.; Kouwer, P. H. J.; Yagi, S.; Mueller, P.; Swager, T. M. *J. Mater. Chem.* **2008**, *18*, 400–407.
- (60) Larew, N. A.; Van Wassen, A. R.; Wetzels, K. E.; Machala, M. M.; Cummings, S. D. *Inorg. Chim. Acta* **2010**, *363*, 57–62.
- (61) Che, C.-M.; Chow, C.-F.; Yuen, M.-Y.; Roy, V. A. L.; Lu, W.; Chen, Y.; Chui, S. S.-Y.; Zhu, N. *Chem. Sci.* **2011**, *2*, 216–220.
- (62) Chen, Y.; Li, K.; Lu, W.; Chui, S. S.; Ma, C. W.; Che, C. M. *Angew. Chem., Int. Ed.* **2009**, *48*, 9909–9913.
- (63) Lu, W.; Roy, V. A.; Che, C. M. *Chem. Commun.* **2006**, 3972–3974.
- (64) Kui, S. C.; Hung, F. F.; Lai, S. L.; Yuen, M. Y.; Kwok, C. C.; Low, K. H.; Chui, S. S.; Che, C. M. *Chem.—Eur. J.* **2012**, *18*, 96–109.
- (65) Yuen, M. Y.; Roy, V. A.; Lu, W.; Kui, S. C.; Tong, G. S.; So, M. H.; Chui, S. S.; Muccini, M.; Ning, J. Q.; Xu, S. J.; Che, C. M. *Angew. Chem., Int. Ed.* **2008**, *47*, 9895–9899.
- (66) Sun, Y.; Ye, K.; Zhang, H.; Zhang, J.; Zhao, L.; Li, B.; Yang, G.; Yang, B.; Wang, Y.; Lai, S. W.; Che, C. M. *Angew. Chem., Int. Ed.* **2006**, *45*, 5610–5613.
- (67) Zhang, Y.; Zhang, H.; Mu, X.; Lai, S. W.; Xu, B.; Tian, W.; Wang, Y.; Che, C. M. *Chem. Commun.* **2010**, *46*, 7727–7729.
- (68) Brunet, E.; Juanes, O.; Jiménez, L.; Rodríguez-Ubis, J. C. *Tetrahedron Lett.* **2009**, *50*, 5361–5363.
- (69) Wilson, M. H.; Ledwaba, L. P.; Field, J. S.; McMillin, D. R. *Dalton Trans.* **2005**, 2754–2759.
- (70) Williams, J. A. G. *Top. Curr. Chem.* **2007**, *281*, 205–268.
- (71) Mydlak, M.; Mauro, M.; Polo, F.; Felicetti, M.; Leonhardt, J.; Diener, G.; De Cola, L.; Strassert, C. A. *Chem. Mater.* **2011**, *23*, 3659–3667.
- (72) Barral, K.; Moorhouse, A. D.; Moses, J. E. *Org. Lett.* **2007**, *9*, 1809–1811.